

# Numerical Study of Steel Structures Responses to External Explosions

Mohammad Abdallah

**Abstract**—Due to the constant increase in terrorist attacks, the research and engineering communities have given significant attention to building performance under explosions. This paper presents a methodology for studying and simulating the dynamic responses of steel structures during external detonations, particularly for accurately investigating the impact of incrementing charge weight on the members total behavior, resistance and failure. Prediction damage method was introduced to evaluate the damage level of the steel members based on five scenarios of explosions. Johnson–Cook strength and failure model have been used as well as ABAQUS finite element code to simulate the explicit dynamic analysis, and antecedent field tests were used to verify the acceptance and accuracy of the proposed material strength and failure model. Based on the structural response, evaluation criteria such as deflection, vertical displacement, drift index, and damage level; the obtained results show the vulnerability of steel columns and un-braced steel frames which are designed and optimized to carry dead and live load to resist and endure blast loading.

**Keywords**—Steel structure, blast load, terrorist attacks, charge weight, damage level.

## I. INTRODUCTION

**D**UE to the increasing awareness of safety concerns for public buildings from intentional or unintentional blast loads and the growing number of domestic regions which suffer from terrorist activities; the analysis and design of blast loads have become a necessity, not only for facilities prone to accidental/chemical explosions but also to any public building in regions subjected to terrorist attacks. Nowadays, many federal agencies and private building owners require buildings to be able to resist the effects of blast loadings [1]. The analysis and design of the structures for blast loads require an understanding of the explosion phenomena and the dynamic responses of the structure. Blasting loads could be defined as the load result from explosions or chemical ammunitions. The threat of bombs depends on two major factors; the bomb size or the charge weight ( $W$ ), and the standoff distance between the explosion source and the target ( $R$ ). Vehicles are considered to be the easiest and most common way to carry out terrorist attacks targeting civilian buildings; for instance the bombing attack on the Australian Embassy in Jakarta (September 2004) and the attack on the HSBC Bank in Istanbul (November 2003). The used charge weight in the both terrorist attacks was approximately 150kg TNT [2]. Estimations on the quantities of explosives in various vehicles

are presented in Table I [3].

In recent years, steel structures are widely used for civilian buildings, and the vulnerability of these kinds of structures to resist blast loading is still a controversial topic. Therefore, some studies have been conducted in this area to investigate the dynamic behavior of steel frame structures to internal explosions [4] and external explosions [5], [6] or steel elements such as columns, beams and connections [7], [8]. Most of these attempts have evaluated the structural response criteria such as deflection and damage level under selected charge weight and standoff distance. However, the blast response of steel members-structures during different scenarios of detonations is necessary to develop an effective strategy to protect building structures against terrorist attacks. This paper examines the steel columns and un-braced steel frames under several blast events, and provides a methodology to simulate the dynamic behavior to carefully assess the blast capacity, resistant ability and failure modes of steel elements during medium-scale explosions. The analysis carried out for five charge weights (100, 200, 300, 400 and 500) kg TNT at 3 m standoff distance. Also, the damage prediction method based on support rotation is introduced to estimate the damage level in each scenario.

TABLE I  
ESTIMATED QUANTITY OF EXPLOSIVES IN VARIOUS VEHICLES

| Vehicle type            | Charge mass / kg |
|-------------------------|------------------|
| Compact car trunk       | 115              |
| Trunk of a large car    | 230              |
| Closed van              | 680              |
| Closed truck            | 2 270            |
| Truck with a trailer    | 13 610           |
| Truck with two trailers | 27 220           |

## II. BLAST LOAD, CHARACTERS AND DETERMINATION

The explosion phenomena can be redacted as a time history profile based on the pressure released from the bomb vs. the diverse time stages. It consists of two periods; the positive and the negative period (Fig. 1). Owing to the fact that the crucial damage ordinarily occurs in the positive phase and the resulting negative pressure is always less than the positive pressure; the negative phase pressure is nullified for analysis and design purposes [9]. In this study only the positive period pressure was taken for analysis purposes. However, most researches dealing with the dynamic behavior of structures under blast loading have attempted to simplify the actual blast load to an effortless one (Fig. 2 (a)). Ding et al. [10] and Astarlioglu et al. [11] used the simplified uniform blast load (Fig. 2 (b)), Hwang [12] during his work on the response of

Mohammad Abdallah is with the College of Engineering, Civil and Architectural Engineering Department, Palestine Polytechnic University, Hebron, Palestine (e-mail: mohammad.mozher@gmail.com).

steel structures under blast loading used the resultant forces at joint points after determining it using CONWEP software (Fig. 2 (c)). Abdallah et al. [9] in their work on evaluating the dynamic responses of steel columns subjected to blast load examined the three cases and they found that the dynamic responses in case (a) and case (b) are extremely close to one another with very little variation.

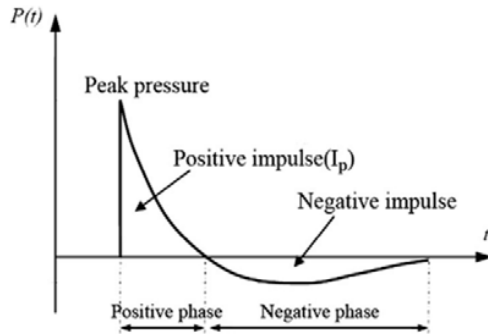


Fig. 1 Blast load time history curve

There are many resources used to determine the blast loads on structures. USA military publications is considered the most widely used, reports worth noting are; a technical report published by Kingery and Bulmash [13], the army technical manual TM5-1300 [14], and Unified Facilities Criteria Publications (UFC) [15], these resources provide a set of charts to calculate blast wave parameters based on the scaling law.

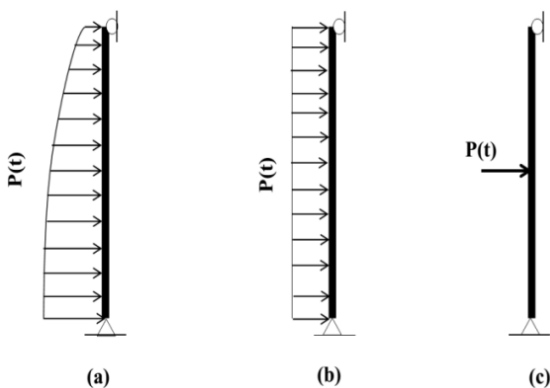


Fig. 2 Applied blast load cases (a), (b), and (c)

Lately, many specialized programs such as CONWEP and ATBLAST, which depend on and adjust with the field data collected from various blast experiments, have emerged and many presumed investigations have used these programs to predict blast loads parameters. ATBLAST is a software program used to estimate the blast loads that develop during a detonation. The program allows for the inputting of a minimum and a maximum range, an explosive charge weight and an angle of incidence and then calculates the shock front velocity, time of arrival, pressure (P), impulse (I) and duration time ( $t_d$ ) [16].

### III. THE STEEL MATERIAL MODEL

The steel material's behavior in dynamic events differs from that of it in elastic analysis due to the high strain rate of loading; rapidly applied loads trigger to increase the steel yield strength and result in the reduced plastic deformation. To simulate the dynamic behavior of steel material under blast loading in the finite element codes; two methods are widely used; the first method depends on applying the dynamic increase factor on the static stress-strain curve and the second one is to use Johnson-cook (J-C) strength and failure model.

#### A. Dynamic Increase Factor (DIF)

For high strain loadings such as blast loading, the stress/strain relation is not widely available when compared to static loadings. One approach to determine the dynamic stress strain relationship is by applying the dynamic increase factor (DIF) to the static relation. The dynamic increase factor, (1), as a function of strain rate  $\epsilon'$  which was introduced by Jones [17], is usually used to determine the effect of strain rate which refers to the ratio of the material's dynamic strength to static strength. TM5-1300 provides a chart (Fig. 3) to determine DIF of A36 steel for design purposes.

$$DIF = 1 + \left( \frac{\epsilon'}{D} \right)^{\frac{1}{q}} \quad (1)$$

where: DIF is dynamic increase factor; D and q are constants for the particular material. For steel  $D = 40$  and  $q = 5$ .

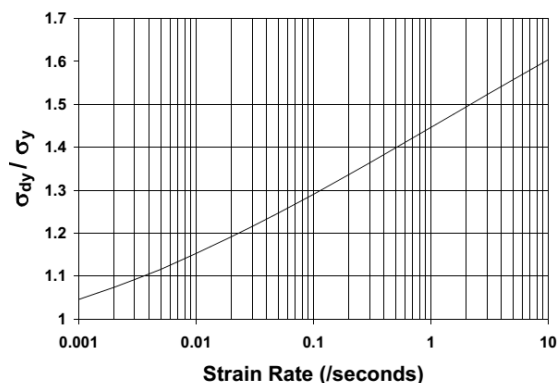


Fig. 3 Dynamic Increase Factor vs. Strain Rate for Yield Stress of A36 Steel

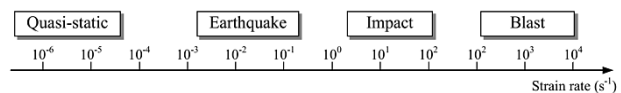


Fig. 4 Strain rates associated with different types of loading

Blast loads typically produce very high strain rates in the range of  $(10^2 - 10^4) S^{-1}$ , as shown in Fig. 4 [18]. Although, some previous field tests have been carried out to accurately determine the average strain rate  $\epsilon'$ , the adequate selection is strongly associated with the explosion and material physical properties and might vary from one test to another. However, to avoid imprecision in representing steel material; the J-C

proposed strength model would be discussed and used in this reported study as described in the following sections.

### B. Johnson–Cook Strength and Failure Model

Johnson-Cook introduced a strength model based on several experiments, (2) [19], which was used recently in an effort to describe the mechanical properties of metal materials that experience high-rated deformation or melting process due to external factors [20].

$$\sigma_y = [A + B(\epsilon_{eff}^p)^N](1 + C \ln \dot{\epsilon})[1 - (T_H)^M] \quad (2)$$

Johnson-Cook in the above equation, which consists of three parts, provides a method to determine the yield stress  $\sigma_y$  from the effective plastic strain  $\epsilon_{eff}^p$  in the first part (where A is the elastic yield stress) and the strain-rate hardening  $\dot{\epsilon}$  in the second part, with including the stress softening caused by high temperature in the last part, where  $T_H$  is a homologous temperature. The equation also contains B, N, C and M as control material parameters. However, the material failure criterion also defined is based on the previous equation by Johnson-Cook [21] and presented in (3).

$$\epsilon^F = \left[ D_1 + D_2 \exp \left( D_3 \frac{P}{\sigma_{eff}} \right) \right] (1 + D_4 \ln \dot{\epsilon}) + D_5 T_H \quad (3)$$

where  $\epsilon^F$  and P are the strain rate at the failure limit and mean stress (pressure) respectively.  $D_1, D_2, D_3, D_4$  and  $D_5$  present the material constant.

### C. Verification of Strength Model

Yuen et al. [22] carried out several field tests for studying the deformation of mild steel plates (ASTM A36) subjected to large-scaled explosions (Fig. 5). Hence, ASTM A36 bears many similarities to steel grade S275 in both chemical and physical properties [23]. In order to verify the acceptance and accuracy of the strength and failure model to use in blast analysis; selected tests have been simulated in ABAQUS and the results were compared to that of those in the experiments. In the experiments of Yuen et al., the targeted steel plates that were used had a size of 500 mm × 500 mm with fully fixed boundaries and 3 mm and 6 mm thickness. The peak blast pressure and time duration were measured during the experiments. The Johnson-Cook strength and failure parameters were included based on the references [24], [25] and tabulated in Table II.

The steel plates were numerically modeled as shell elements in ABAQUS/Explicit finite element analysis software [26], as shown in Fig. 6. It is common and suitable to use this program for transient dynamic events such as blast and impact problems because of its ability to use explicit dynamic finite element formulation. Explicit dynamic analysis and S4R material type have been selected. S4R is a fully integrated general purpose conventional shell element in ABAQUS and it accounts for finite membrane strains and arbitrarily large rotations, which makes it suitable for large-rotation problems. The S4R element is a four-node element. Each node has three displacement and three rotation degrees of freedom.

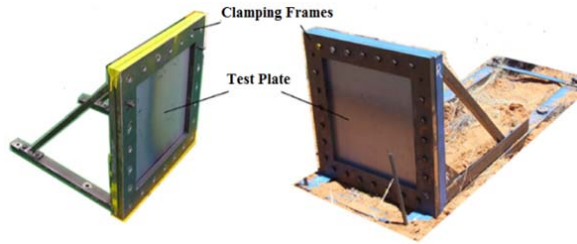


Fig. 5 Yuen tests steel plates

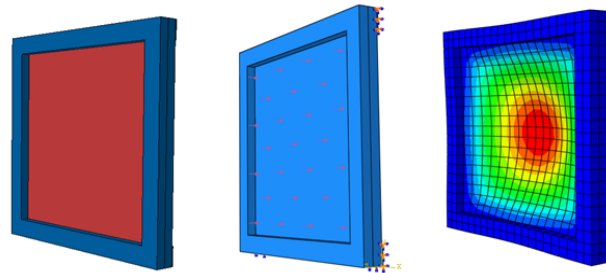


Fig. 6 The modeling of steel plates subjected to blast load

The ABAQUS/Explicit analysis with Johnson-Cook method gave similar results to that of the experimental results; the error percentages between the actual deformations to that obtained from the numerical analysis were calculated and are represented in Table III. This convergence between the results emerges from the material properties were considered in the J-C model as the failure criterion, the material control constants and the included strain rate. Errors might have arisen due to the material values and the implemented boundary conditions but were small enough to ignore. The results of this case study have verified the proposed material strength model in its use in the next steel elements simulations.

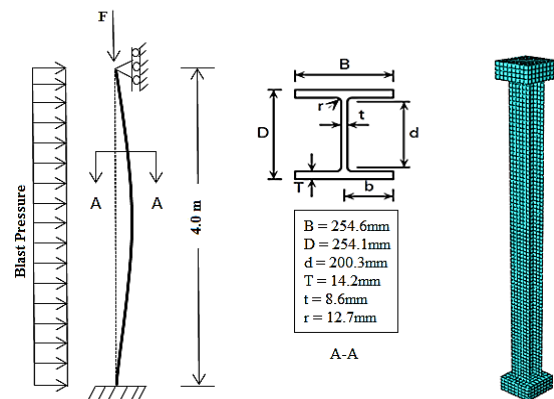


Fig. 7 Geometric configuration and loading of column under explosion

## IV. AXIALLY LOADED COLUMNS SUBJECTED TO EXPLOSION

Fig. 7 shows an axially loaded steel column (S275) with the cross section and boundary conditions details. Column length of 4 m is considered in this section to study the dynamic response of steel columns and to assess the column's damage

level due to varied scenarios of explosions. The steel column was numerically modeled as shell element using ABAQUS finite element code. Explicit dynamic analysis and S4R material type have been selected. A rigid block was connected to each end of the steel column model to avoid inauthentic

distortion on the boundary. The boundary constraints are applied on the rigid block surfaces. An axial compression load ( $F = 0.3P_{cx}$ ) is applied on the top steel plate, where  $P_{cx}$  is the compression resistance of the column about the major axis.

TABLE II  
MATERIAL PARAMETERS

| Density* | $\nu$ | A (ksi) | B (ksi) | N     | C      | M     | $T_M^{**}$ | $T_R^{***}$ | $\dot{\epsilon}_0(sec^{-1})$ |
|----------|-------|---------|---------|-------|--------|-------|------------|-------------|------------------------------|
| 7860     | 0.3   | 41.5    | 72.54   | 0.228 | 0.0171 | 0.917 | 1500       | 20          | 1.0                          |
| $D_1$    | $D_2$ | $D_3$   | $D_4$   | $D_5$ | -      | -     | -          | -           | -                            |
| 0.0705   | 1.732 | -0.54   | -0.015  | 0.0   | -      | -     | -          | -           | -                            |

Note: \*Density in  $kg/m^3$ , \*\* $T_M$ : melt temperature in  $^{\circ}C$ , \*\*\* $T_R$ : reference temperature in  $^{\circ}C$

TABLE III  
COMPARISON BETWEEN THE TESTS MEASURED RESULTS AND J-C METHOD  
(NUMERICALLY)

| Test no. | Thickness (mm) | Z*   | Pressure (kPa) | $t_d^{**}$ (ms) | $\delta_{test}$ | $\delta_{ABAQ.}$ | Error % J-C |
|----------|----------------|------|----------------|-----------------|-----------------|------------------|-------------|
| 1        | 3              | 1.28 | 582.05         | 7.73            | 28.60           | 26.76            | 6.43        |
| 2        | 3              | 0.83 | 1495.98        | 3.53            | 40.70           | 43.33            | 6.46        |
| 3        | 3              | 0.79 | 1634.19        | 8.99            | 50.90           | 50.60            | 0.59        |
| 4        | 3              | 0.72 | 1993.45        | 5.95            | 60.60           | 56.50            | 6.60        |
| 5        | 6              | 1.05 | 908.25         | 8.71            | 18.10           | 18.14            | 0.22        |

Note: \*Z: scaled distance  $kg/m^3(1/3)$ , \*\* $t_d$ : peak pressure duration time in ms.

#### A. Static Analysis, Compression Capacity

So, as to determine the column's ultimate vertical capacity; the steel column was firstly modeled in ABAQUS program without blast loads. The axial load is applied as a static load on the top steel plate surface and increased through specific time interval. The load was defined as a ramp function, starting from zero until it reaches its maximum limit. A load increment of 200 kN/s is added until the buckling stage is obtained. The whole loading process lasts 13 sec. The column's ability to resist vertical load is up to 2521 kN, after that, a catastrophically irreversible buckling occurs eliminating the column's vertical resistance, as in Fig. 8.

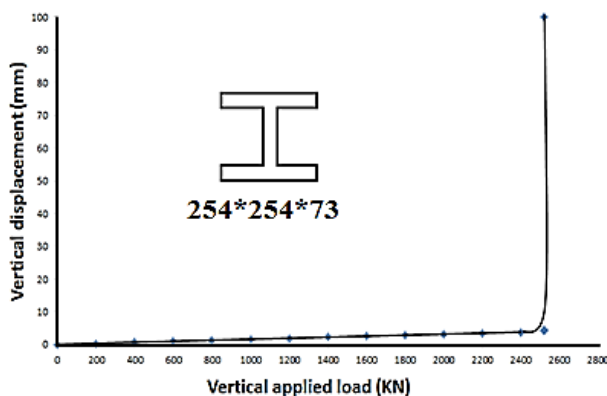


Fig. 8 Vertical capacity of steel column

This vertical capacity value ( $P_{cx}$ ) could be calculated by BS 5950-1:2000 code, the cross section capacity usually being checked by:

$$\frac{F_c}{A_g P_y} + \frac{M_x}{M_{cx}} + \frac{M_y}{M_{cy}} \leq 1 \quad (4)$$

where  $F_c$ ,  $P_y$ ,  $A_g$ ,  $M_x$ ,  $M_{cx}$ ,  $M_y$  and  $M_{cy}$  are the applied axial load, cross-sectional area, yield stress, maximum major axis moment, major axis moment capacity, maximum minor axis moment and minor axis moment capacity, respectively. For this column  $A_g P_y$  is equal to 2560.25 KN.

#### B. Dynamic Analysis, Blast Response

The impact of different charge weights at a 3 m standoff distance was investigated. In each scenario, the transfer blast loads (reflected pressure) were calculated at the mid-height point of the steel column using the ATBLAST program, thereafter, the uniform pressure distributed on the exposed surface. To avoid the column weak situation and because column stiffness plays a main role to resist transverse load [27], the major axis surface was chosen to exposure blast pressure.

In order to verify the acceptance of ATBLAST results; the analytical method, which is explained in UFC publications, was used to determine the blast reflected pressure in the case where the charge weight is 100kg. The ATBLAST result at the steel column's mid-height is 12,474.13 kPa and 12,430.00 kPa by using the analytical method (UFC), the margin for error is less than 1% (relative to ATBLAST results). Table IV shows the blast pressure and time duration for each case.

The load has been divided into two steps. In the first step, the applied axial load is starting from zero up to its maximum value during 50 ms and was maintained constant thereafter until the end of the analysis. In the second step, the transverse blast reflected pressure started when the axial load had reached its maximum value. The time step duration was 400 ms for the whole analysis (Fig. 9)

Considering all of the aforementioned data, dynamic/explicit analyses are carried out for each charge weight. A closer look was taken at energy findings to check if hour-glass distortion was a problem in the case of the selected element type (S4R) and mesh size in each blast scenario.

Hour-glass is a spurious deformation mode resulting from the excitation of zero-energy degree of freedom which could easily destroy the simulation. Fig. 10 shows the artificial strain energy which is less than 5% of the total internal energy for the column in S1. Also, the figure shows the comparison

between the external work and the total internal energy. The results show the level of hour-glass distortion is acceptable and assert the reasonable accuracy of the assumed mesh size and material type.

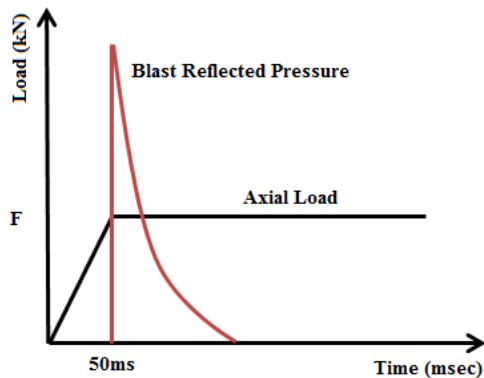


Fig. 9 Applied load steps

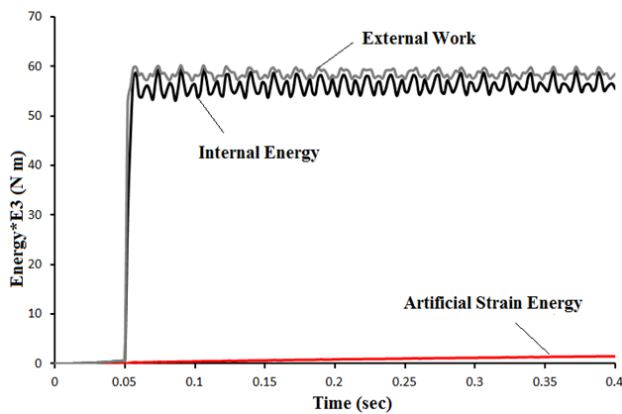


Fig. 10 Energy results of the steel column in S1

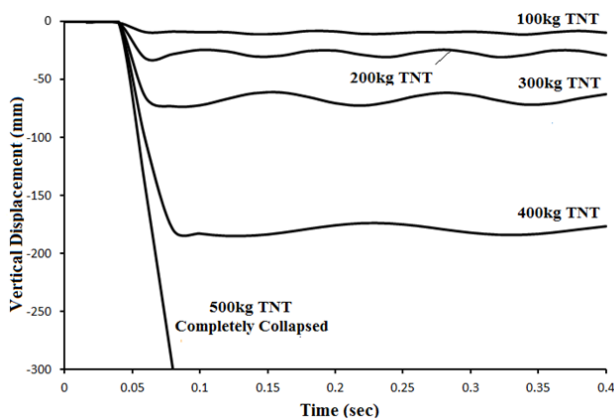


Fig. 11 Responses of axially loaded column subjected to explosion

The response curves of the column during the varied explosions scenarios are shown in Fig. 11. It appears that the top support displacement of the steel column increased dramatically when the charge weight exceeded 100 kg TNT. The maximum vertical displacement when the charge weight

was equivalent to 100 kg TNT is 11.47 mm and then increased to 30.90 mm, 73.23 mm and 184.84 mm when the charge weight changed to 200 kg, 300 kg and 400 kg, respectively, while the column completely collapsed at 500 kg TNT charge weight. The vertical displacement might give an indication about the column's damage and bulking which could be used to evaluate the damage level as would be discussed in the next section.

### C. Damage Assessment

The damage patterns and modes depend basically on different significant parameters such as the applied load type, load intensity and the material properties. In the blast load and steel material case; shear damage model is predicted to happen, as well as flexural damage model. The irreversible buckling due to blast pressure intensity with shear damage is observed as shown in Fig. 12. The blast loads (S1 to S4) caused permanent deformation on the column in the form of out-of-straightness with magnitude equivalent to 2.03%, 4.87%, 8.69% and 15.2% of the column length, respectively.

Damage of steel members could be determined by investigating support rotation. The support rotation value  $\theta$  can be determined based on the maximum structure deformation and its length as defined by (5) [28]. The maximum allowable deformation depends on the protection level; occupants and equipment (category 1) and the component itself (category 2). The limit of these categories are  $2^\circ$  and  $12^\circ$ , respectively.

$$\theta = \tan^{-1}\left(\frac{\delta_{mid}}{0.5L}\right) \quad (5)$$

where  $\theta$ ,  $\delta_{mid}$  and  $L$  are the maximum support rotation, the midpoint displacement of columns and the column height, respectively.

Table V demonstrates the detailed analysis to predict the column's damage level. The table shows the vulnerability of the steel column to resist blast loading; 100 kg TNT at 3 m standoff distance was great enough to make the column unstable with significant damage and irreversible buckling values ( $\theta > 2$ ).

TABLE IV  
EXPLOSION SCENARIOS

| Scenario # | Charge weight kg TNT | Standoff distance m | Reflected pressure kPa | Time Duration ms |
|------------|----------------------|---------------------|------------------------|------------------|
| S1         | 100                  | 3.00                | 12474.13               | 0.71             |
| S2         | 200                  | 3.00                | 20942.27               | 0.71             |
| S3         | 300                  | 3.00                | 26890.17               | 0.76             |
| S4         | 400                  | 3.00                | 31915.35               | 0.81             |
| S5         | 500                  | 3.00                | 36343.58               | 0.86             |

This response could trigger to local or total collapses of the entire building, especially if the axial load ratio is being greater than 0.3. However, the support rotation increased up to  $16.90^\circ$  with high damage level when the charge weight increased to 400kg TNT before being totally destroyed at 500 kg TNT.

TABLE V  
THE COLUMN DETAILED ANALYSIS RESULTS

| Scenario # | Charge weight in kg TNT | Displacement* in mm | $\theta$ | Limit C2* | Comment              |
|------------|-------------------------|---------------------|----------|-----------|----------------------|
| S1         | 100                     | 81.14               | 2.32°    | 12°       | Low Damage           |
| S2         | 200                     | 194.70              | 5.56°    | 12°       | Medium Damage        |
| S3         | 300                     | 347.60              | 9.86°    | 12°       | Medium-High Damage   |
| S4         | 400                     | 607.80              | 16.90°   | 12°       | High Damage-collapse |
| S4         | 500                     | -----               | -----    | 12°       | Totally collapsed    |

\*Midpoint displacement. C2 = Category two

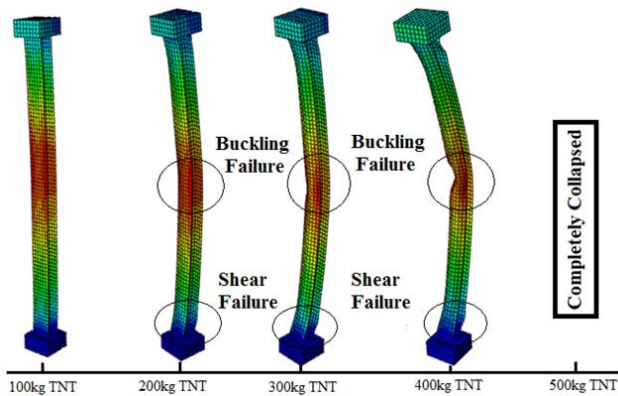


Fig. 12 Column response and collapse patterns

#### V. UN-BRACED STEEL FRAME SUBJECTED TO EXPLOSIONS

A rigid steel frame in structural engineering could be defined as the load-resisting skeleton constructed with straight or curved members interconnected by mostly rigid connections which could resist movements induced at the members joints. Fig. 13 shows a fourth story rigid steel frame of a typical building, which was considered in this reported section. Each floor has a height of 4 m. There are four spans in the X direction with 6 m length each. The total height of the steel frame is 16 m and the total X width is 24 m. The steel frame members (S275) were designed and optimized to carry the dead and live load (gravity load) based on BS 5950-1 code [29], [30]. Columns-beams joints are assumed to be rigid joints.

The reflected blast pressure at the mid height of each floor for the different charge weights at 3 m standoff distances have been calculated and then distributed on the column's outer surface as a uniform pressure. Fig. 14 shows the calculated blast pressure produced from 100kg TNT along the frame elevation.

To study the dynamic responses of rigid steel frame under blast loading, and because of frames in real constructions have been already subjected to gravity load (dead and live load) before any terrorist attacks, the load has been applied in two steps. In the first step, the gravity load (Q) started from zero up to maximum value during 50 ms and was maintained constant thereafter up to the end of analysis. In the second step, and because the steel frame consists of four floors, the blast load has been divided into four intervals depending on the duration time of blast wave. The time at 50 ms is

considered the starting point for applying the blast pressure, as shown in Fig. 15.

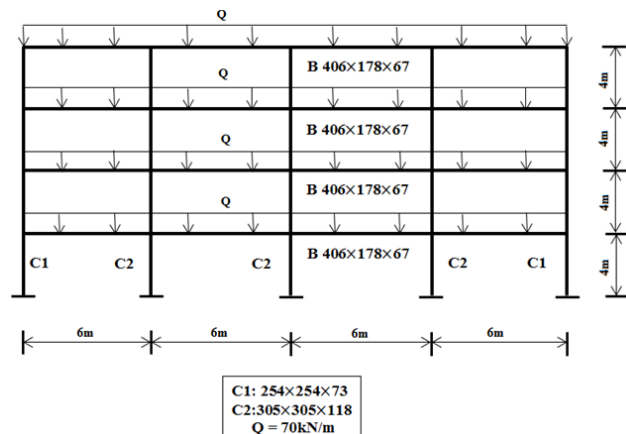


Fig. 13 Four-storey frame

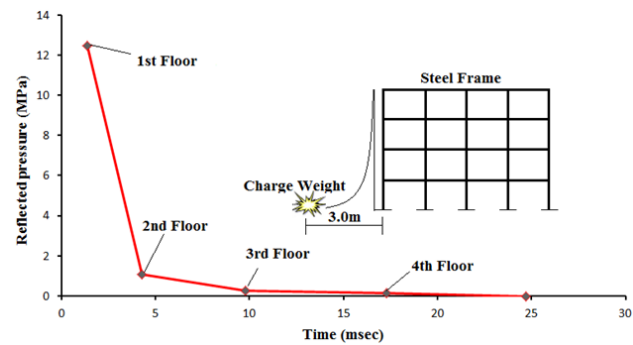


Fig. 14 Reflected pressure

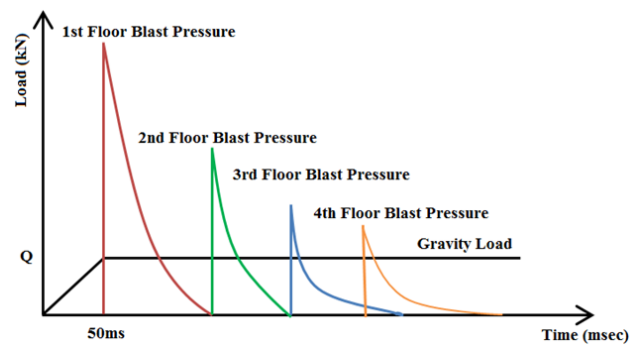


Fig. 15 Applied load sequences

Dynamic/explicit analyses with J-C strength model and S4R selected material type are carried out on the frame under the five explosion scenarios (S1-S5) to study the dynamic frame behavior. The frame's members were numerically modeled as the shell element in ABAQUS. However, the responses of the vertical displacement at the left edge of the top floor are presented in Fig. 16. The results indicate that although the charge is redoubled to 500 kg TNT, the structure would not totally collapse. But obviously, the frame members experienced significant damage when the mass exceeded 100



kg. The maximum vertical displacement increased dramatically to 106.84 mm when the charge weight was 500 kg.

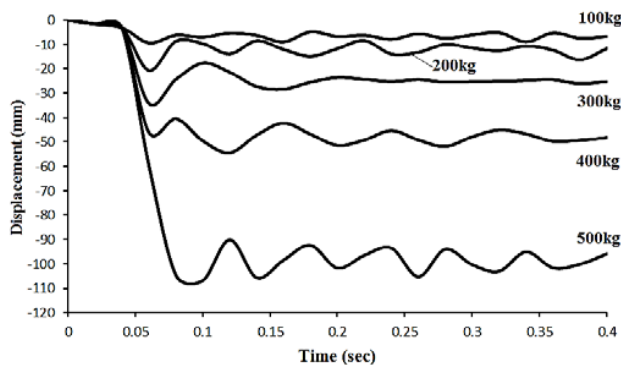


Fig. 16 Responses of frame under explosions

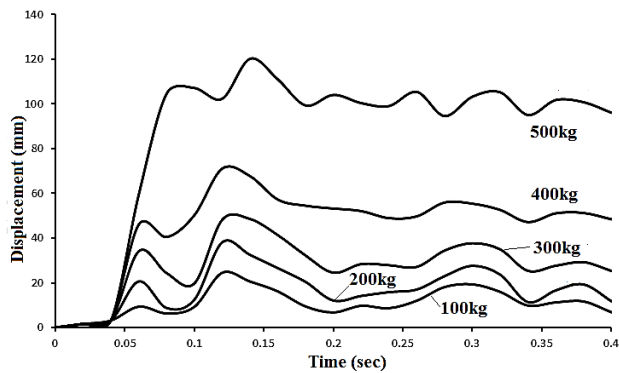


Fig. 17 Frame's drift

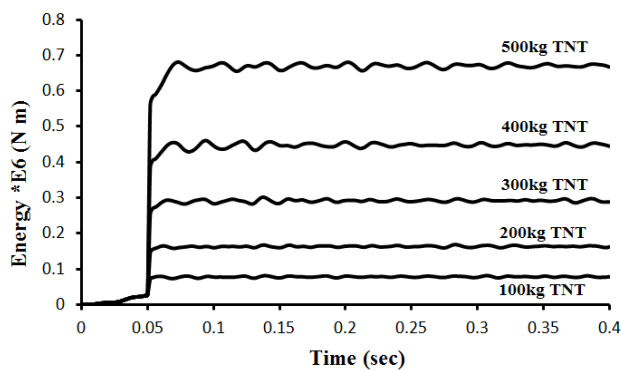


Fig. 18 External work of the frame against explosions

Nevertheless, a closer look was taken at the total frame sway to recap its ability to resist and endure blast loading. The frame drift at the left edge of the top floor (Fig. 17) shows the vulnerability of gravity load design to resist blast load. The drift index could be defined as the ratio of the maximum deflection at the top of the building to its total height. It is accepted up to 1/500 [31]. The drift index usually has to be included during analysis and design procedures to satisfy the structural stability. Here, the drift index values show the

failure of the steel frame to resist detonation greater than 100 kg TNT at 3 m standoff distance. The steel frame drift index in the blast scenarios (S1-S5) was equal to 0.0015, 0.0024, 0.0030, 0.0044 and 0.0075, respectively.

External work could be used as another method for better understanding the frame's behavior based on the work done against the explosion. Fig. 18 shows the frame's external work curves during the detonation's scenarios. It is observed that the external work done by the frame is approximately increased twice by adding 100 kg TNT in each trial. The obtained external work was around 80.27 E3 Nm, 164.11 E3 Nm, 293.30 E3 Nm, 450.46 E3 Nm and 680.92 E3 Nm in S1, S2, S3, S4 and S5, respectively.

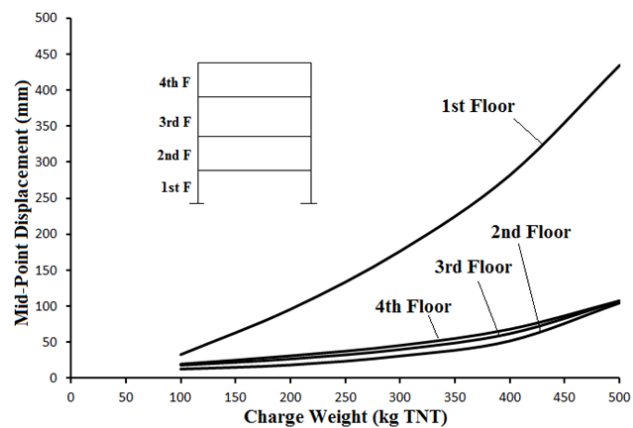


Fig. 19 Mid-point displacements of the left side columns

With regard to evaluating the frame damage level, the maximum mid-point displacement of the outer columns along the left frame elevation has been calculated (Fig. 19). These displacements might be used to recap the damage level in each story. However, the findings show that the outer columns of the 2<sup>nd</sup>, 3<sup>rd</sup> and 4<sup>th</sup> floor have approximately the same mid-point displacement under the same charge weight, whilst a vast gap is observed in the results of the 1<sup>st</sup> floor column. For instance, when the charge weight is 300kg TNT, the obtained maximum mid-displacement was 176.67 mm, 31.02 mm, 40.08 mm and 45.7 mm for the 1<sup>st</sup>, 2<sup>nd</sup>, 3<sup>rd</sup> and 4<sup>th</sup> floor, respectively. In addition, the increasing of the charge weight up to 500kg TNT at 3 m standoff distance has no major effect on the columns mid-point displacement, except the first floor's column. This means that the lowest and nearest part to the charge position has proven to receive the majority of the blast impact and pressure because the effective distance from the explosion source to any point on the frame depends heavily on the standoff distance and the point height. Fig. 20 illustrates the collapse mode of the 1<sup>st</sup> floor column under 500 kg TNT at 3m standoff distance.

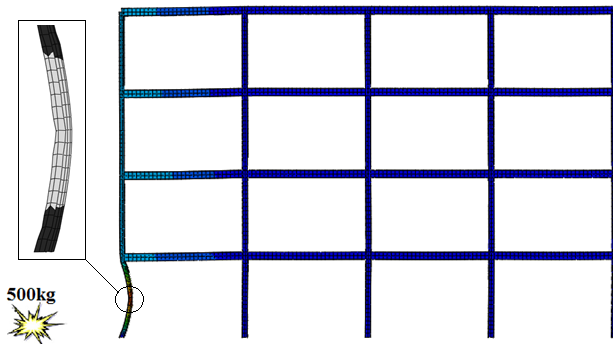


Fig. 20 Typical in-plane frame's response

## VI. CONCLUSIONS

Because all of the current design codes have no particular guidelines regarding the analysis and design of steel buildings to blast loading, a methodology to evaluate the dynamic response of steel column and rigid frame subjected to explosions has been introduced through different charge weights at 3 m standoff distance. The analyses were carried out to carefully evaluate the dynamic response of steel members due to moderate detonations. Different methods were used to determine the blast pressure, and experimental results were used to verify the acceptance of proposed steel strength and failure model, and to calibrate the ABAQUS finite element code for blast loading analysis.

The external explosions have proven to have a catastrophic impact on the steel elements stability. A blast from 100 kg TNT was great enough to make an axially loaded column unstable with a significant damage level and irreversible buckling value ( $\theta > 2$ ). Also, the dynamic/explicit analysis proved the vulnerability of the steel structure with gravity load design to resist moderate explosions. The drift index value was in the unacceptable range when the detonation's mass is greater than 100kg of TNT.

Moreover, it is shown that the influence of charge weight increasing strongly concentrates on the columns near to detonations, whilst no major changes have been reported in the remaining columns. This might highlight the key point to develop an effective strategy to protect civilian buildings against terrorist attacks by carrying out further intensive analytical and experimental studies on the adjacent members' under more scenarios to generalize and then prevent collapses and sever failures.

## REFERENCES

- [1] National Research Council (NRC), Protecting People from Bomb Damage: Transfer of Blast-Effects Mitigation from Military to Civilian Applications, National Academy Press, Washington, DC, (1995).
- [2] Remennikov, A. Carolan, D. (2005). Building vulnerability design against terrorist attacks. In M. Stewart, B. Dockrill (Eds.). // Proceedings of the Australian Structural Engineering Conference 2005, pp. 1-10, Australia: Tour Hosts Pty. Ltd.
- [3] Hrvoje Draganić, Vladimir Sigmund, Blast Loading on Structures, Djelovanje eksplozivnih konstrukcija. // Tehnički vjesnik. 19, 3(2012), pp. 643-652.
- [4] B.M. Luccioni, R.D. Ambrosini, R.F. Danesi. Analysis of building collapse under blast loads. // Engineering Structures. 26, (2004), pp. 63-71.
- [5] J.Y. Richard Liew, Survivability of steel frame structures subject to blast and fire. // Journal of Constructional Steel Research. 64, (2008), pp. 854-866.
- [6] Zhang Xiuhua, Duan Zhongdong and Zhang Chunwei, Numerical Simulation of Dynamic Response and Collapse for Steel Frame Structures Subjected to Blast Load. // Trans. Tianjin Univ. 14, (2008), pp. 523-529.
- [7] Tapan Sabuwala, Daniel Linzell, Theodor Krauthammer, Finite element analysis of steel beam to column connections subjected to blast loads. // International Journal of Impact Engineering. 31, (2005), pp. 861-876.
- [8] Girum S. Urgessan, Tomasz Arciszewski, Blast response comparison of multiple steel frame connections. // Finite Elements in Analysis and Design. 47, (2011), pp. 668-675.
- [9] Mohammad Abdallah, Bashir H. Osman. A methodology for evaluating dynamic responses of steel columns subjected to blast load under different situations. // The IES Journal Part A: Civil & Structural Engineering, (2015).
- [10] Ding, Y., M. Wang, Z. X. Li, H. Hao.. Damage Evaluation of the Steel Tubular Column Subjected to Explosion and Post-explosion Fire Condition. // Engineering Structures. 55, (2013), pp. 44-55.
- [11] Astarlioglu, S., T. Krauthammer, D. Morency, and T. P. Tran. Behavior of Reinforced Concrete Columns under Combined Effects of Axial and Blast-Induced Transverse Loads. // Engineering Structures. 55, (2013), pp. 26-34.
- [12] Hwang, Y. S. Three Dimensional Responses of a Steel Structure under Blast Loads. // PhD thesis, University of Southern California. 2010.
- [13] Kingery C. N., Bulmash G. Technical report ARBRL-TR-02555: Air blast parameters from TNT spherical air burst and hemispherical burst. AD-B082 713, U.S. Army Ballistic Research Laboratory, Aberdeen Proving Ground, MD. (1984).
- [14] U.S. Department of the Army. Structures to resist the effects of accidental explosions. // Technical Manual (1990), pp. 5-1300.
- [15] Unified Facilities Criteria. UFC 3-340-02 Structures to Resist the Effects of Accidental Explosions. // U.S. Army Corps of Engineers, Naval Facilities Engineering Command, Air Force Civil Engineer Support Agency. (2008).
- [16] ARA. Products, Software, Blast Design Software, A.T.-Blast. Applied Research Associates: <http://www.ara.com/products/AT-blast.htm>. (2014).
- [17] Jones N. Structural impact. Cambridge, New York: Cambridge University Press; 1988.
- [18] Ngo, T. Mendis, P. Gupta, A. & Ramsay, J. Blast Loading and Blast Effects on Structures - An Overview. // EJSE Special Issue: Loading on Structures. (2007)
- [19] Johnson GR, Cook WH. A constitutive model and data for metals subjected to large strains, high strain rate and high temperatures. // Proceeding of the 7th international symposium on ballistics, Hague, Netherlands, (1983).
- [20] Yuen SCK, Nurick GN. Experimental and numerical studies on the response of quadrangular stiffed plats. Part I: subjected to uniform blast load. // Int J Impact Eng. 31, (2005), pp. 55-83.
- [21] Johnson GR, Cook WH. Fracture characteristics of three metals subjected to various strains, strain rates, temperatures and pressures. // Eng Fract Mech. 21, 1(1985), pp. 31-48.
- [22] Yuen SCK, Nurick GN, Verster W, et al. Deformation of mild steel plates subjected to large-scaled explosions. // Int J Impact Eng. 35, (2008), pp. 684-703.
- [23] Leeco Steel. S275 Steel Plates, URL: <http://www.leecosteel.com/s275-steel-plate.html>
- [24] Schwer L. Optional strain-rate forms for the Johnson Cook constitutive model and the role of the parameter Epsilon. // Proceeding of the 6th LS-DYNA Anwenderforum, Frankenthal, German; (2007).
- [25] Seidt JD. EOD material characterization, supplemental reports: constitutive and fracture models for ASTM A36 hot rolled steel. Battelle Technical report prepared for the Naval Explosive Ordnance Disposal Technology Division, Columbus, Ohio; (November 2005).
- [26] Dassault Systèmes Simulia Corp. Abaqus Version 6.13-1, Abaqus Analysis User's Manual, Abaqus Keywords Reference Manual, Abaqus Example Problems Manual, Dassault Systèmes Simulia Corp. (2013).
- [27] M. M. Abdallah, B. H. Osman. Advanced Materials and Structural Engineering. // Proceedings of the International Conference on Advanced Materials and Engineering Structural Technology (ICAMEST). (2015), Qingdao, China.
- [28] Mays, G. C., and P. D. Smith. Blast Effects on Buildings Design of



Buildings to Optimize Resistance to Blast Loading. London: Tomas Telford. (1995).

- [29] Structural use of steelwork in building, BS 5950-1:2000, Part 1: Code of practice for design, Rolled and welded sections, (May 2001).
- [30] The British Constructional Steelwork Association Ltd and the Steel Construction Institute, Hand book of structural steel work 4th edition. (2007).
- [31] Bryan Stafford Smith, Alex Coull. Tall Building Structures: Analysis and Design. Awiley-Interscience Publication, USA. (1991).